British Journal of Pharmacology (2008) 154, 1649–1661

0007–1188/08 $30.00
www.brjpharmacol.org

RESEARCH PAPER

CO-MP4, a polyethylene glycol-conjugated haemoglobin derivative and carbon monoxide carrier that reduces myocardial infarct size in rats

KD Vandegriff[1], MA Young[1], J Lohman[1], A Bellelli[2], M Samaja[3], A Malavalli[1] and RM Winslow[1,4]

[1]*Sangart, Inc., San Diego, CA, USA;* [2]*Department of Biochemical Sciences, University of Rome 'La Sapienza', Piazzale Aldo Moro 5, Rome, Italy;* [3]*Department of Medicine, Surgery and Dentistry, Ospedale San Paolo, University of Milan, Milan, Italy and* [4]*Department of Bioengineering, University of California, San Diego, CA, USA*

Background and purpose: MP4 (Hemospan) is a Hb-based oxygen therapeutic agent, based on polyethylene-glycol (PEG) conjugation to Hb, undergoing clinical trials as an oxygen carrier. This study describes the functional interaction between MP4 and carbon monoxide (CO), as a CO delivery agent, and the effects of CO-MP4 on myocardial infarct size following ischaemia and reperfusion in rats.
Experimental approach: Kinetic measurements of CO-MP4 binding were used to evaluate the effects of PEG modification on Hb subunit structure/function and to calculate CO-MP4 equilibrium constants. CO transport by CO-MP4 was shown by ligand (O_2/CO) partitioning between MP4 and red blood cell (RBC)-Hb. Pharmacological effects of CO-MP4 were studied on myocardial infarction in rats.
Key results: CO binding kinetics show primary structural/functional effects on β chains in MP4, with α chains maintaining the ability to undergo tertiary conformational transition. CO confers long-term, room-temperature stability and is able to rapidly re-equilibrate between MP4 and RBCs. In a rat model of myocardial infarct, in contrast to oxy-MP4, CO-MP4 reduced infarct size when administered prior to the induction of ischaemia.
Conclusions and implications: MP4 PEGylation chemistry modifies the individual function of Hb subunits, but results in an overall CO equilibrium constant similar to that for unmodified Hb. CO-MP4 is able to deliver CO to the circulation and reduces ischaemia/reperfusion injury in rats, providing the first evidence for this drug as a CO therapeutic agent.
British Journal of Pharmacology (2008) **154,** 1649–1661; doi:10.1038/bjp.2008.219; published online 9 June 2008

Keywords: Hemospan; MP4; CO-MP4; poly(ethylene) glycol-conjugated Hb; blood substitute; carbon monoxide; myocardial infarct

Abbreviations: IHP, inositol hexaphosphate; LR, lactated Ringer's solution; MP-11, microperoxidase-11; PBS, phosphate-buffered saline; PEG, polyethylene glycol; PC, preconditioning

Introduction

Hemospan, also referred to in research literature as MP4, is an oxygen therapeutic agent that has completed phase I (Björkholm *et al.*, 2005) and phase II (Olofsson *et al.*, 2006, 2008) clinical trials, with phase III trials currently underway in Europe. The Hb-based product is made by conjugation of approximately 7 polymers of 5-kD maleimide-activated poly(ethylene) glycol (PEG) to human Hb (Acharya *et al.*, 1996; Vandegriff *et al.*, 2003). The molecule has been well characterized; the protein/polymer chemistry is associated with unique physicochemical properties, including high O_2 affinity and low cooperativity (Vandegriff *et al.*, 2003), increased rates of O_2 dissociation, assigned to the β subunits (Vandegriff *et al.*, 2004), and an increased radius of gyration and maximal molecular dimensions compared to unmodified human Hb (Svergun *et al.*, 2008). Mounting evidence points to local perturbations of the β-subunit haem pocket in MP4, although the solution structure by small-angle X-ray scattering revealed no differences in Hb tertiary structure at a resolution of approximately 12-Å (Svergun *et al.*, 2008).

Although Hemospan is being developed as an O_2 carrier, the action of MP4 as a carbon monoxide (CO) carrier (that is, CO-MP4) is also under exploration. First, the increased stability of the bond between the haem iron and CO, with respect to that with O_2, implies that the CO-Hb complex is more stable than oxy-Hb by inhibition of autoxidation. This is expected to translate into increased stability of CO-MP4 during storage because of the absence of Hb oxidation to methemoglobin (met-Hb). Second, CO is now recognized

Correspondence: Dr KD Vandegriff, Sangart Inc., 6175 Lusk Blvd., San Diego, CA 92121, USA.
E-mail: kvandegriff@sangart.com
Received 27 December 2007; revised 11 February 2008; accepted 9 May 2008; published online 9 June 2008

as a cell signalling molecule with cytoprotective and vasodilator actions in models of cardioprotection (Fujimoto *et al*., 2004; Guo *et al*., 2004; Stein *et al*., 2005), vasodilation (Motterlini *et al*., 2002; Foresti *et al*., 2004), inflammation (Sawle *et al*., 2005) and haemorrhage/resuscitation (Otterbein, 2002; Kubulus *et al*., 2005; Zuckerbraun *et al*., 2005).

Carbon monoxide inhalation studies have provided primary evidence for the beneficial actions of exogenous CO administration (Nakao *et al*., 2003, 2005; Fujimoto *et al*., 2004; Neto *et al*., 2004; Zuckerbraun *et al*., 2005; Belcher *et al*., 2006; Kohmoto *et al*., 2007), but the arterial CO-Hb levels reached in these studies are potentially unsafe (Mirza *et al*., 2005; Durante *et al*., 2006; Gautier *et al*., 2007). Studies by Motterlini and colleagues (Clark *et al*., 2003; Guo *et al*., 2004; Stein *et al*., 2005) suggest that controlled and targeted delivery of CO is more feasible with intravenous delivery of CO-releasing molecules. These findings lead to the new concept that transfusing CO-Hb derivatives might add a new function to Hb-based O_2 carriers, for example, as CO-delivery agents. The dual purpose of this study was (1) to describe the CO ligand binding function of this PEGylated Hb, CO-MP4, and (2) to examine the pharmacological effects of CO-MP4 on myocardial infarct size in rats through CO delivery.

Materials and methods

CO binding kinetics

Laser photolysis and stopped-flow, rapid-mixing experiments were carried out in 0.1 M HEPES buffer, 0.1 M Cl^- at pH 7.4 and 23 °C. The buffer solution was equilibrated under 1 atm of CO gas at 23 °C, giving a stock CO solution of 1.05 mM. Hb and MP4 samples were diluted directly into this buffer to form the CO derivatives. The CO buffer solution was also used after dilution with degassed buffer to obtain the final CO concentration. Microperoxidase mixing experiments were carried out in phosphate-buffered saline (PBS) (10 mM phosphate, 0.1 M Cl^-), pH 7.3 at 25 °C.

Laser photolysis experiments

Carbon monoxide rebinding time courses on submicrosecond to millisecond time scales following laser photolysis were measured to determine geminate rebinding and relaxed-conformation ('R-state') association reactions, respectively. The Hb concentration was 3 μM (in haem) diluted in 1 atm CO-equilibrated HEPES buffer at room temperature. Data were acquired following photolysis by a 5-ns flash from an Nd-YAG laser (Quanta Systems HIL 101, Milan, Italy, second harmonic wavelength $\lambda = 532$ nm and 80 mJ $pulse^{-1}$). The energy was tuned to approximately half that for these experiments. Maximal photolysis obtainable with the set-up was approximately 50% after geminate rebinding, presumably due to the duration of the pulse being significantly shorter than the tumbling time of Hb, which causes the extinction coefficient (that is, the probability of absorbing a quantum) of the polarized laser light to be lower than that measured under continuous illumination. Transmittance was monitored at 436 nm, the isosbestic point for deoxy T- and R-state Hbs, using a system with an Oriel 150-W arc lamp, a Spex 1681 monochromator and a Hamamatsu H6870 photomultiplier tube, set orthogonal to the laser beam, amplified with either a 5-MHz Hamamatsu C1053 current-to-voltage amplifier for microsecond resolution or a 300-MHz Analog Modules A353 amplifier for nanosecond resolution. All output was fed to a Tektronix TDS360 digital oscilloscope. Kinetic traces were time-averaged to reach suitable signal-to-noise levels for evaluation.

On the millisecond time scale following photolysis, CO diffuses out of the haem pocket and into the solvent. Partial photolysis time courses were collected at decreasing levels of breakdown. Laser power was reduced until ⩽10% breakdown of the fully liganded Hb was obtained. Under these conditions, the only reaction being monitored is: $Hb_4(CO)_3 + CO \rightarrow Hb_4(CO)_4$, which gives association rate constants for 'R-state' Hb. Time courses were fitted to a two-exponential expression with equal amplitudes to distinguish rates of binding to α and β subunits, according to Olson and co-workers (Mathews and Olson, 1994; Unzai *et al*., 1998):

$$\Delta A_t = 0.5 \cdot \Delta A_0 \cdot [e^{(-kf \cdot t)} + e^{(-ks \cdot t)}] \quad (1)$$

where ΔA_t is the absorbance change at time t, ΔA_0 is the total change in absorbance at $t = \infty$, and k_f and k_s are the observed fast and slow first-order rate constants, respectively. All fitting was performed using an iterative, non-linear least squares algorithm in MATLAB (The Math Works Inc., Natick, MA, USA). Bimolecular association rate constants were obtained by dividing the observed rates by the CO concentration: $(k' = k_{obs}\,[CO]^{-1})$.

'R-state' dissociation kinetics by rapid mixing using a ligand displacement reaction

Rates of CO dissociation were measured in a stopped-flow, rapid-mixing apparatus (Applied Photophysics, MV17, Leatherhead, UK). A stock nitric oxide (NO) solution was prepared in a 20-mL syringe containing degassed water, equilibrated at 20 °C with 1 atm of NO gas ([NO] = 2 mM at 20 °C). This solution was diluted 10- and 40-fold for final NO concentrations of 200 and 50 μM in buffer solution, containing approximately 1 mg of solid sodium dithionite to eliminate any trace of O_2. CO-Hb solutions were prepared from degassed buffer mixed with buffer equilibrated at 1 atm of CO at a ratio of 2:1, giving a CO concentration of approximately 330 μM, again with approximately 1 mg of added dithionite to scavenge any extraneous O_2. This CO-equilibrated buffer was diluted 10-fold in the Hb solutions, giving final concentrations of 6 μM Hb-CO in solution containing approximately 33 μM CO before mixing. Thus, the [NO]/[CO] experimental reaction ratios were approximately 6 and 1.5. The disappearance of Hb-CO was monitored by absorbance changes at 420 nm. Three kinetic traces were averaged per run. The time courses were fitted to the two-exponential expression in Equation (1) to evaluate subunit differences. If the time courses were determined to be monophasic, they were fit to a single-exponential expression given as follows:

$$\Delta A_t = \Delta A_{max} \cdot [1 - e^{(-k \cdot t)}] \quad (2)$$

'R-state' dissociation kinetics by CO competitive binding with microperoxidase-11

Microperoxidase-11 (MP-11) is a partly digested haem protein with a haem group bound to 11 amino acids that binds CO faster and stronger than Hb (Sharma and Ranney, 1982; Samaja *et al*., 1987). The stock solution of MP-11 (MP-11$^+$ oxidized form, Sigma Chemicals, St Louis, MO, USA, MP-11, M6756) was prepared daily at 0.25 mM concentration in PBS, pH 7.3 at 25 °C. A 3-mL, 1-cm quartz cell with a magnetic stirrer was filled with 1.9 mL of stock MP-11$^+$ and a few crystals of Na-dithionite to reduce it to MP-11 and placed in a diode-array spectrophotometer (Agilent HP 8453, Santa Clara, CA, USA). The reaction was started at 25 °C by adding 0.1 mL Hb at a final concentration of 0.025 mM ([MP-11]/[Hb] = 10) and recorded for 200 s at 1-Hz sampling. In experiments with inositol hexaphosphate (IHP), IHP was added to the cell before mixing at a ratio [IHP]/[Hb tetramer] = 5. Spectra analysis (data not shown) indicated that the best wavelength to follow the CO competitive binding was 590 nm, with the following ε ($mM^{-1}\,cm^{-1}$): CO-Hb = 2.48, deoxy-Hb = 7.12, deoxy-MP-11 = 0.36 and CO-MP-11 = 0.65. Unconstrained data were fitted assuming one-phase exponential association (that is, first order reaction) using Equation 2.

'T-state' association kinetics by rapid mixing

The kinetics of CO association to the deoxygenated Hb were measured by a stopped-flow, rapid mixing (Applied Photophysics, MV17). The Hb solutions were prepared by diluting the protein in deoxygenated HEPES buffer and adding ~0.1 mg mL^{-1} of Na-dithionite immediately prior to the measurements to ensure complete removal of O_2 from the buffer. The Hb samples were mixed with the CO solutions (100, 50 and 25 μM before mixing), and the reactions were monitored for the disappearance of deoxy-Hb at 436 nm. The Hb concentration was 6 μM (in haem, before mixing) to maintain pseudo-first-order conditions. Three kinetic traces were averaged per run. Under the experimental conditions used here, CO combination is irreversible, and the off rate constants can be ignored. However, if the Hb undergoes allosteric transition, the time course of CO binding to deoxy-Hb is cooperative, with four independent binding sites. However, these complicated time courses cannot be analysed for four rate constants because of large uncertainties in the fitted parameters. Therefore, to simplify analysis, a single-exponential equation (Equation (2)) was used to fit Hb time courses to obtain the slower tense-conformation ('T-state') rate. A double-exponential expression was required to fit the MP4 time courses in which the spectral amplitudes of the two phases were allowed to vary:

$$\Delta A_t = y \cdot [\Delta A_0 \cdot e^{(-kf \cdot t)}] + (1 - y) \cdot [\Delta A_0 \cdot e^{(-ks \cdot t)}] \qquad (3)$$

where ΔA_t is the absorbance change at time t, ΔA_0 is the total change in absorbance at $t = \infty$, y = fractional amplitude for the fast phase, and k_f and k_s are the observed fast and slow first-order rate constants, respectively. The bimolecular rate constants were obtained by dividing the observed rate constants by the CO concentration after mixing: ($k' = k_{obs}$ $[CO]^{-1}$).

CO equilibrium constants

'R-state' CO equilibrium constants were calculated as $K_R = k'\ k^{-1}$, where the overall constant is given by:

$$K_R = \sqrt{K_{R\alpha} K_{R\beta}} \qquad (4)$$

where $K_{R\alpha}$ and $K_{R\beta}$ are R-state equilibrium constants for α and β subunits, respectively.

Size-exclusion chromatography

Oxygenated Hb (oxy-Hb) and oxy-MP4 samples were prepared at decreasing stock concentrations [2.6, 0.06 and 0.015 mM (in haem)], diluted in PBS, pH 7.4 and analysed by size-exclusion chromatography using an AKTA Purifier-10 (FPLC) (Amersham/Pharmacia, Piscataway, NJ, USA), with two Superose columns in series. To induce full tetramer dissociation into dimers, the proteins (2.6 mM, in haem) were eluted in the presence of 0.9 M $MgCl_2$. Samples were eluted at a flow rate of 0.5 mL min^{-1} at room temperature. Detection was performed at 540 nm using a 0.5-cm flow-through cell. Eluted concentrations were measured using $\varepsilon_{540} = 13.5\ mM^{-1}\,cm^{-1}$.

CO-MP4 storage stability

The storage stability of CO-MP4 was measured as the percent formation of met-Hb over time. Oxy-MP4 was converted to the fully saturated CO form by gently blowing 1 atm of CO gas over the surface of the solution in a fume hood. The CO product was sealed in a glass bottle under an atmosphere of CO. CO-MP4 and oxy-MP4 samples were stored at 37 °C for 30 days. Samples were removed from the bottles at timed intervals and tested for percent met-Hb by co-oximetry (IL CO-oximeter 682, Lexington, MA, USA).

CO transport from CO-MP4: ligand redistribution between MP4 and RBC-Hb

Either air- or CO-equilibrated human blood ([Hb] ~160 g L^{-1}) was mixed with either CO- or air-equilibrated MP4 at the product's formulated concentration ([MP4] ~40 g L^{-1}), respectively. The mixtures were performed at a 1:1 ratio (v/v) for 30 min at room temperature to simulate a 50% exchange transfusion. At the end of mixing, the samples were centrifuged, and the supernatant was removed and stored for analysis. The pelleted RBCs were washed three times in PBS and re-suspended in PBS in the same volume of supernatant that was removed. The supernatant (MP4) and RBC compartments were analysed separately for percent CO-Hb by co-oximetry.

Rat model of myocardial ischaemia and reperfusion injury

All animal procedures and protocols were approved by the Sangart IACUC, and the studies were performed at Sangart, Inc. Male Sprague-Dawley rats (260–322 gm) were fasted overnight, anaesthetized with pentobarbital sodium (50 mg kg^{-1}, i.p.), intubated and mechanically ventilated ($FiO_2 = 0.3$) to maintain eucapnia. Catheters were placed in

one femoral artery and vein for measurement of arterial pressure and infusion of test substances, respectively. The heart was exposed, and a 6-O silk suture placed around the left anterior descending coronary artery at the level of the left atrial appendage, making a snare together with a flared piece of PE50 tubing. A thermocouple was placed in the thoracic cavity to continuously record temperature. Phasic and mean arterial pressure and thoracic temperature were continuously displayed and recorded at 100 Hz using a BioPac MP100 data acquisition unit (BIOPAC Systems, Inc., Goleta, CA, USA). Heart rate for each beat was calculated as the reciprocal of the interval between successive pressure peaks and averaged each minute.

Arterial blood samples ($\sim$200 μL) were collected from the arterial catheter into heparinized microhematocrit tubes and analysed immediately for PO_2, PCO_2, pH using a Bayer 248 blood gas analyzer. Total Hb and plasma Hb were measured using HemoCue B- and Plasma/low Hb photometers (HemoCue AB, Ängelholm, Sweden). Haematocrit was measured after centrifugation. The fraction of oxy-Hb, CO-Hb and met-Hb was measured by co-oximetry using extinction coefficients for rat blood.

Five groups of animals were studied randomly: lactated Ringer's (LR, $n=13$); CO-MP4 (low dose, $n=10$); CO-MP4 (high dose, $n=10$); oxy-MP4 ($n=10$); and preconditioning (PC) as a positive control ($n=5$). For LR, oxy-MP4 and low-dose CO-MP4, an infusion equivalent to 10% of blood volume was begun 5 min prior to coronary ligation and delivered over 35 min (0.2 mL kg^{-1} min^{-1}). After 30 min, the occlusion was released, and the infusion rate of test solution was slowed to 0.54 mL kg^{-1} hr^{-1} to deliver the equivalent of 20% of blood volume during the ensuing 24 h. In the high-dose CO-MP4 group, the initial infusion was 20% of blood volume over 35 min, followed by 30% of blood volume over the ensuing 24 h. Animals in the PC group were subjected to three 5-min coronary occlusions, separated by 5 min, prior to the 30-min index ischaemia and received LR according to the LR regimen described above. Following release of the coronary ligation, the thoracic thermocouple was removed, the chest closed in layers, and the animals weaned from the ventilator. The arterial and venous cannulae were tunnelled subcutaneously, exited at the interscapular space and the animals jacketed to protect the catheters. The animals were replaced in their original housing cage with a tether attached to the jacket for continuous intravenous infusion of test material over 24 h of recovery. Blood samples were collected at baseline, immediately following release of the coronary ligation and 24 h after release of the ligation for co-oximetry, haematocrit, Hb and plasma Hb.

After 24 h of recovery, blood samples were collected, and the animals received 100 units of heparin i.v. and were euthanized with an overdose of euthanasia solution, Euthasol (Virbac, Fort Worth, TX, USA). The heart was removed, the aorta cannulated and the heart perfused retrograde via the aorta with LR on a Langendorff apparatus. The coronary snare was then tied to re-occlude the vessel, and the non-ischaemic tissue was delineated by perfusion with 1% Evans blue dye. The atria and right ventricle were removed, and the left ventricle was sliced into 2-mm rings beginning at the apex and placed in 1% triphenyl tetrazolium chloride (37 °C for 15 min), followed by overnight immersion in 10% neutral buffered formalin. Heart slices were photographed digitally. Total left ventricle area, area at risk, and infarct area were measured using NIH ImageJ, 1.37v, by an investigator without knowledge of the treatment group.

Statistics

Data are presented as mean and s.e.m. Infarct size was analysed by analysis of covariance with area at risk as the covariate, followed by Student's *t*-test with Bonferroni's correction for four comparisons (Kusuoka and Hoffman, 2002). All other data from animal studies were analysed for differences between means using a one-way analysis of variance with correction for multiple comparisons. Differences from baseline within a group were tested using Dunnett's test. Statistical analyses were performed using GraphPad Instat 3 (GraphPad Software) or JMP (SAS Institute, Cary, NC, USA) statistical software.

Materials

Human Hb and MP4 were prepared as described previously (Vandegriff *et al*., 2003). Reagents of the highest purity available were obtained from Sigma Chemicals (St Louis, MO, USA). Maleimide-activated PEG was provided by NOF (Tokyo, Japan). Hb concentrations were measured using a diode array spectrophotometer (Agilent HP 1853, Santa Clara, CA, USA), using the extinction coefficient at 523 nm = 7.12 mM^{-1} cm^{-1} (Snell and Marini, 1988). Met-Hb levels were $\leqslant$3%.

Results

CO association kinetics

Geminate binding. Following photolysis, the reaction scheme is as follows:

$$\text{CO-Hb} \leftrightarrow \text{Hb.CO} \leftrightarrow \text{Hb} + \text{CO} \quad (5)$$

Over the submicrosecond time course, we neglected bimolecular rebinding and spontaneous dissociation of CO in the dark, which simplifies the post-flash time course scheme to

$$\text{CO-Hb} \leftarrow \text{Hb.CO} \rightarrow \text{Hb} + \text{CO} \quad (6)$$

For Hb, the yield of photolysis was approximately 50%, and the geminate yield was approximately one-third of the total absorbance change (Figure 1). The observed rate constant of 15 μs^{-1} equals the sum of the rate constants of geminate rebinding and ligand exit to the solvent. As the observed geminate yield is the ratio between the two processes, we estimate that the effective geminate rebinding to Hb occurs at 5 μs^{-1}, and the escape of the photolyzed ligand to the solvent at 10 μs^{-1}. In marked contrast to Hb, MP4 showed no CO geminate rebinding phase.

'R-state' association. Rate constants for the bimolecular recombination of CO were determined by partial laser flash

photolysis by reducing laser power. Geminate rebinding from within the haem pocket is complete by $t > 250$ ns, after which partial photolysis produces a fraction of unliganded haems that composes 10–20% of the total haems, thus making the most populated Hb R-state derivatives $Hb(CO)_4$ and $Hb(CO)_3$. Under these experimental conditions, the observed rebinding time course can be ascribed almost entirely to the $Hb_4(CO)_3$ species. Time courses at all powers of laser photolysis (Figures 2a and b) are shown for the CO association to Hb and MP4. The time courses fit equally well to either single- or double-exponential equations. In this case, the data were fitted to a two-exponential expression using Equation (1) to tentatively distinguish binding between globin chains (Figure 2c). The difference in rates within either Hb or MP4 is small and not highly resolved, but both fast and slow rates for MP4 are approximately 30% higher compared to the respective rates for Hb. The fitted rate constants (k') are reported in Table 1. The rates for Hb are similar to previously reported rates for native Hb (Mathews *et al*., 1989; Unzai *et al*., 1998).

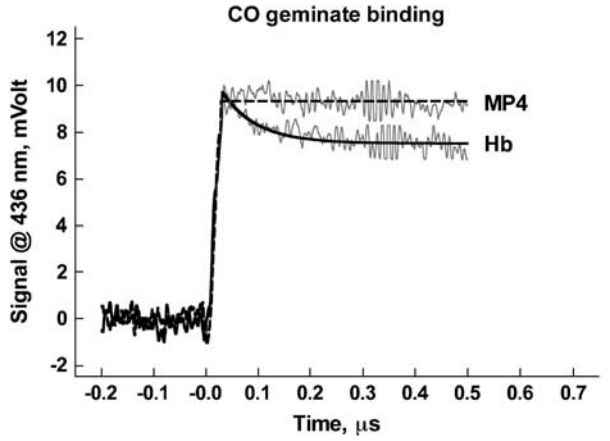

Figure 1 CO geminate binding to Hb (lower trace) and MP4 (upper trace). Solid and dashed lines show the respective fits. CO, carbon monoxide.

'T-state' association. Normalized time courses for the combination of CO to deoxygenated Hb and MP4 at three concentrations of CO are shown in Figures 3a and b. Each time course is an average of duplicate runs at the same [CO]. After mixing, [CO] was 17-, 8- and 4-fold higher than [Hb] (that is, 3 μM in haem), and a pseudo-first-order approximation was used to determine the rates. The averages of the fitted bimolecular rate constants (k') from all time courses are given in Table 1. In stopped-flow experiments to measure the combination of CO with the deoxygenated Hbs, a cooperative Hb will start the reaction in the T state and progressively switch to the R state, showing autocatalysis. This was observed in the time courses for CO binding to deoxygenated Hb (Figure 3a). 'T-state' rates are defined empirically as rate constants for the first step of ligand binding. Under the conditions of our experiment, we determined the best-fit apparent rate for unmodified Hb of $0.23 \pm 0.01\ \mu M^{-1}\ s^{-1}$ ($n = 3$). This value is similar to but slightly higher than rates

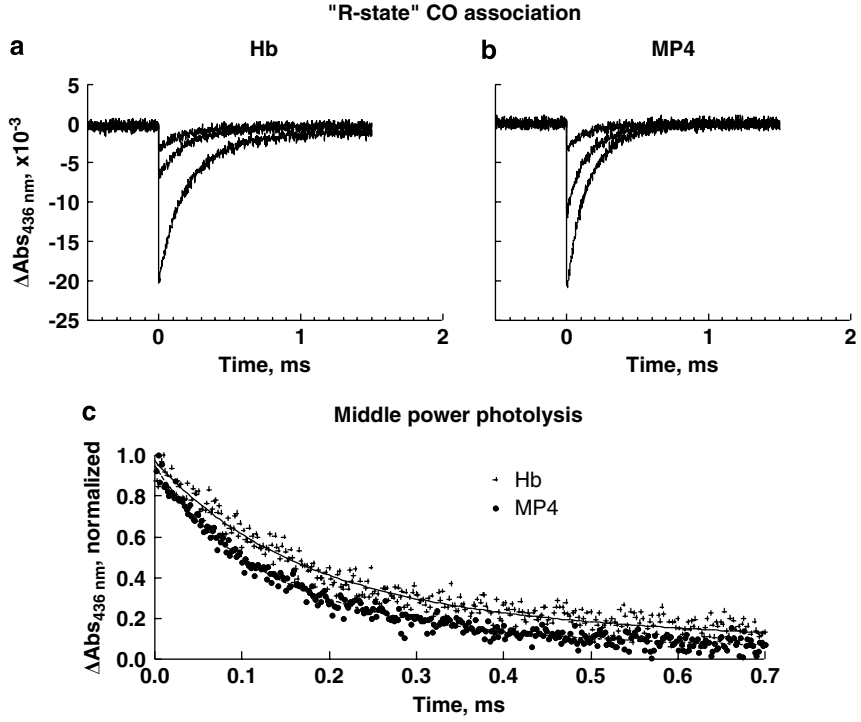

Figure 2 'R-state' CO association to Hb (**a**) and MP4 (**b**), with curves shown at decreasing power from laser photolysis, from bottom to top. (**c**) shows the normalized CO rebinding time courses following partial photolysis for Hb and MP4; both curves were taken from the middle-power photolysis shown in (**a**) and (**b**). The solid lines show fitted curves from Equation (1). Fitted results for the rates are shown in Table 1. CO, carbon monoxide.

Table 1 Kinetic analysis of CO association and dissociation rates for Hb and MP4

		Hb	*MP4*
CO association rates			
Geminate binding	k', μs^{-1}	5	0
'R-state' CO association rates from partial photolysis experiments	k'_s, $\mu M^{-1} s^{-1}$	2.9	4.1
	k'_f, $\mu M^{-1} s^{-1}$	9.0	12.0
'T-state' CO association by rapid mixing with CO	k'_s, $\mu M^{-1} s^{-1}$	0.23 ± 0.01	0.38 ± 0.04
	k'_f, $\mu M^{-1} s^{-1}$		4.44 ± 1.57
CO dissociation rates			
'R-state' CO dissociation from NO displacement	k_s, s^{-1}	0.019 ± 0.001	0.022 ± 0.001
	k_f, s^{-1}		0.032 ± 0.003
'R-state' CO dissociation by competition with MP-11	k, s^{-1}	0.015 ± 0.001	0.016 ± 0.001
	+ IHP	0.024 ± 0.001	0.017 ± 0.001

Abbreviations: CO, carbon monoxide; IHP, inositol hexaphosphate; MP-11, microperoxidase-11.
Laser photolysis and rapid mixing reactions were carried out in 0.1 M HEPES buffer, 0.1 M Cl^- at pH 7.4 and 23 °C. The MP-11 reaction was performed in PBS, pH 7.4 at 25 °C at a final concentration of 0.025 mM ([MP-11]/[Hb] = 10); in IHP experiments, IHP was added at a ratio [IHP]/[Hb tetramer] = 5. Fitted biphasic rate constants for fast and slow phases are denoted k'_f and k'_s, respectively, for association rates, and as k_f and k_s, respectively, for dissociation rates.

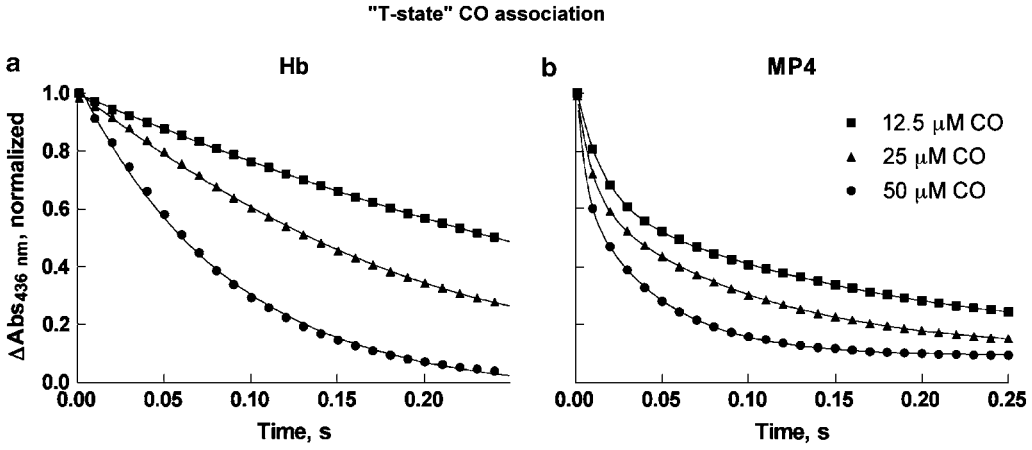

Figure 3 'T-state' normalized time courses of CO association to Hb (**a**) and MP4 (**b**). Time courses were measured by mixing the deoxygenated Hbs (6 μM in haem before mixing) with buffer containing CO at 100, 50 or 25 μM before mixing. Only data sampled every 10 ms are shown for clarity. The solid lines show fits of the data using Equation (3). Fitted rates are given in Table 1. CO, carbon monoxide.

previously assigned to α and β chains in 'T-state' Hb, based on studies with mutant and native humans Hbs (0.12 ± 0.03 and $0.18 \pm 0.05\ \mu M^{-1} s^{-1}$, respectively) (Mathews *et al*., 1991) or studies with metal hybrids (0.16 ± 0.03 and $0.07 \pm 0.02\ \mu M^{-1} s^{-1}$, respectively) (Unzai *et al*., 1998). Subunit rate assignments could not be made in this experiment with native Hb.

In marked contrast to Hb, MP4 time courses were clearly biphasic with a fast rate 10-fold higher than the slow rate (0.38 ± 0.04 and $4.44 \pm 1.57\ \mu M^{-1} s^{-1}$ ($n = 5$)) (Figure 3b; Table 1). The fitted amplitudes of the two phases of MP4 were allowed to vary according to Equation 3, and the amplitude of the fast phase varied between 40 and 45% of the total (versus a theoretical value of 50%). The apparent rates at the three CO concentrations used in these experiments give $t_{1/2}$ values of 12.5, 6 and 3 ms, respectively. Thus, with an apparatus mixing dead time of about 3 ms, it is highly likely that 5–10% of the fast-phase amplitude was lost in mixing, giving a 50:50 ratio in kinetic phases. To support the view that the two reaction phases have equal amplitudes, we observed that the total amplitude for MP4 was less than that for Hb at the same protein concentrations in non-normalized time courses (data not shown). By analogy to unmodified Hb, we assign the lower rate constant for MP4 ($\sim 0.4\ \mu M^{-1} s^{-1}$) to a fraction of 'T-state' MP4 haems, and the higher rate ($\sim 4\ \mu M^{-1} s^{-1}$) to a fraction of 'R-state' haems that are restricted from forming the 'T state'.

By combining the partial photolysis studies and stopped-flow results, we calculate three CO association rate constants for MP4, that is, 12, 4 and $0.4\ \mu M^{-1} s^{-1}$. The $12\text{-}\mu M^{-1} s^{-1}$ phase appears to be lost to a great extent in the dead time of the stopped flow, with the remainder mixed within the $4\ \mu M^{-1} s^{-1}$ phase.

CO dissociation kinetics

'R-state' dissociation by ligand displacement. Representative time courses for CO dissociation in the presence of excess NO ([NO]/[CO] ≅ 6) are shown in Figure 4 (left panel). As all haems have bound ligand during the entire course of the experiment, and the rate-limiting step is CO dissociation, the kinetics provide information on the CO off rate from 'R-state' Hb. All time courses measured at either 6- or 1.5-fold molar excess NO were fitted using Equation 1, and the

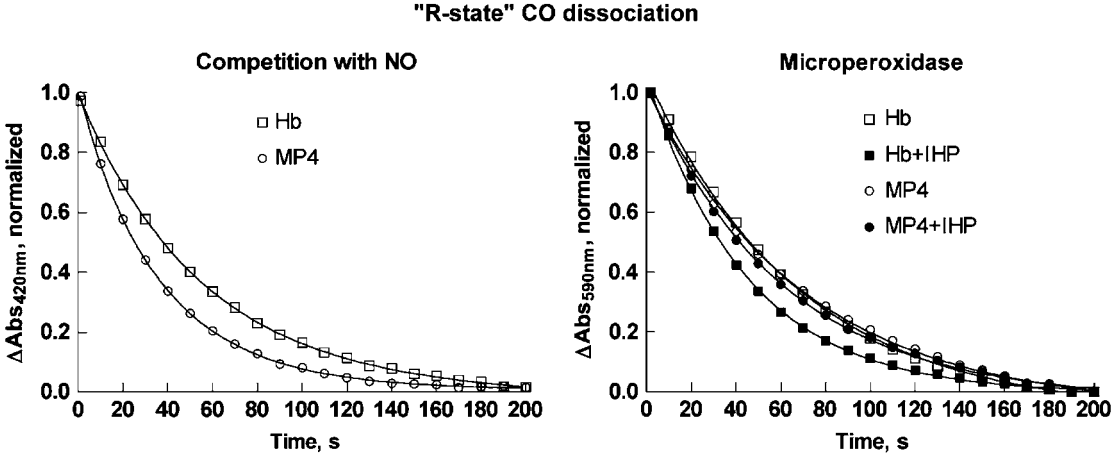

Figure 4 'R-state' CO dissociation from Hb and MP4. The left panel shows the time courses measured by rapid mixing of CO-Hb and CO-MP4 with deoxygenated buffer containing 200 μM NO. Time courses were measured by the change in absorbance at 420 nm and normalized. Only data sampled every 10 s are shown for clarity. The solid lines show the fits using Equation (1), and the rates are given in Table 1. The right panel reports the time courses measured by reaction of CO-Hb and CO-MP4 with MP-11. Experiments in the presence of IHP at a five-fold molar ratio are shown by the closed symbols. Time courses were determined by the change in absorbance at 590 nm and normalized. Solid lines show the fits using Equation (2), and the fitted rates are reported in Table 1. CO, carbon monoxide; IHP, inositol hexaphosphate; NO, nitric oxide.

average rate constants are provided in Table 1. The Hb time course was best fit by a single-exponential equation. In contrast, the MP4 time course showed two kinetic phases. The slow rate is the same as the single rate for Hb, and the fast rate is 50% higher.

'R-state' dissociation by CO competitive binding. The reactions for CO competitive binding to Hb versus MP-11 are as follows:

$$\text{CO-Hb} \rightarrow \text{Hb} + \text{CO} \quad (7)$$

$$\text{Hb} + \text{CO} \rightarrow \text{CO-Hb} \quad (8)$$

$$\text{MP-11} + \text{CO} \rightarrow \text{CO-MP-11} \quad (9)$$

Reaction 9 ($k' \sim 10\,\mu\text{M}^{-1}\,\text{s}^{-1}$) is faster than reaction 8 for [MP-11]/[Hb] > 5 (Samaja *et al*., 1987). Therefore, reaction 7 is the rate-limiting step. Representative time courses are shown in Figure 4 (right panel), and fitted rates are reported in Table 1. The fitted values for k are similar, although slightly less, than those reported for the 'R-state' dissociation as measured in the presence of excess NO, perhaps due to the different buffer conditions. For Hb in the presence of IHP, the rate of the CO dissociation reaction increased by 60%. In contrast, the rate for the MP4 reaction did not change in the presence of this allosteric effector. The latter finding is in agreement with a study showing that βCys93 maleimidation interferes with the IHP effector mechanism of R-state binding (Khan *et al*., 2001).

Dimer formation is attenuated in MP4 solutions

Hb and MP4 dissociations were analysed by size-exclusion chromatography both as a function of Hb concentration and under fully dissociating conditions (Figure 5). As concentration was lowered from ~40 to 1.0 to 0.2 μM (in haem), calculated from the elution peak absorption at 540 nm, unmodified oxy-Hb showed a clear and substantial shift towards decreasing molecular weight. Forced dissociation of oxy-Hb in 0.9 M $MgCl_2$ shifted the peak even further to αβ dimers. Decreasing concentrations of oxy-MP4 show that MP4 is dissociable by the appearance of smaller PEGylated species as descending shoulders on the major peak of the chromatograms, but the shift is highly attenuated compared to Hb, and free αβ dimers could not be resolved at the elution position of fully dissociated Hb (~28 mL) at the lowest concentration of MP4 measured. On the other hand, free αβ dimers were clearly resolved in MP4 under fully dissociating conditions (arrow in Figure 5), but made up <1% of the total species.

CO-MP4 storage stability

Formation of met-Hb in CO-MP4 versus oxy-MP4 was measured over 30 days of storage at 37 °C (Figure 6). While oxy-MP4 oxidized to met-Hb at a rate of 29% day^{-1}, CO-MP4, as expected, did not oxidize and showed a small decline in met-Hb formation over time.

CO transport from CO-MP4 to human RBC-Hb

The ability of CO to partition between intra- and extracellular Hb compartments in mixtures of MP4 at a [Hb] ~40 g L^{-1} and human blood at [Hb] ~160 g L^{-1} was tested in two experiments. In the first (MP4→RBC), CO-MP4 was mixed with air-equilibrated human blood; in the second (RBC→MP4), CO-equilibrated blood was mixed with air-equilibrated oxy-MP4. After 30 min of mixing at room temperature, the samples were separated into RBC and supernatant (that is, plasma MP4) compartments by centrifugation that were then analysed for percent CO-Hb (Figure 7). In both experiments, CO bound initially either to MP4 or RBC-Hb re-equilibrated equally between

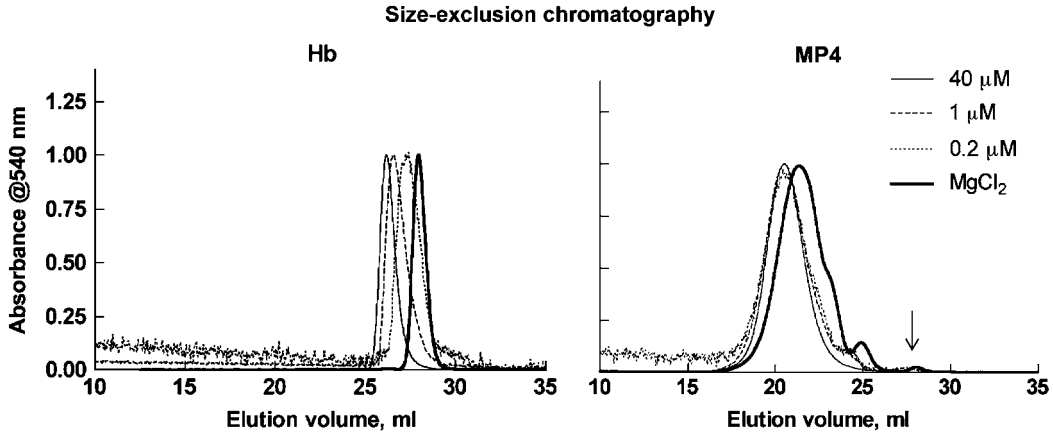

Figure 5 Size-exclusion chromatography of oxy-Hb (left) and oxy-MP4 (right) at decreasing Hb concentrations in PBS and under dissociating conditions in 0.9 M $MgCl_2$ (bold solid line). Stock concentrations in PBS were 2.6, 0.06 and 0.015 mM (in haem). Final eluted concentrations were approximately 40, 1 and 0.2 μM (in haem), respectively, based on the eluted peak absorbances at 540 nm. Traces were normalized for clarity. Shifts to longer retention times reveal decrease in size due to formation of αβ dimers. Species eluting at the free αβ dimer position in MP4 under dissociating conditions are shown by the arrow. PBS, phosphate buffer saline.

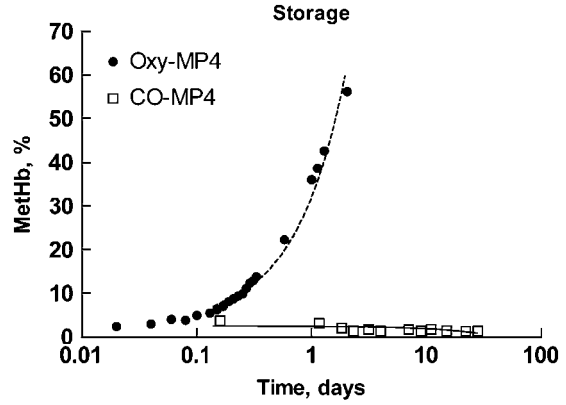

Figure 6 Semi-log plot of met-Hb formation in O_2- and CO-liganded MP4 at 37 °C. The slopes of the best fits are 29.0 ± 0.9% and −0.06 ± 0.03% per day for oxy-MP4 and CO-MP4, respectively ($r^2 = 0.32$ versus 0.98, $P = 0.04$ versus < 0.0001). CO, carbon monoxide.

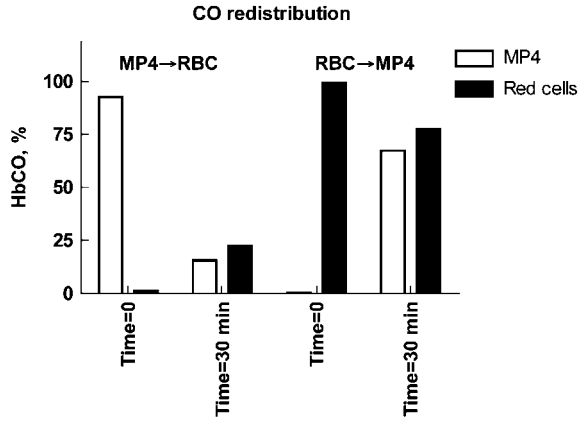

Figure 7 CO re-distribution between MP4 ([Hb] ~40 g L^{-1}) and red cells ([Hb] ~160 g L^{-1}). In MP4→RBC, CO-equilibrated MP4 was mixed 1:1 (v/v) with human blood. In RBC→MP4, CO-equilibrated blood was mixed 1:1 (v/v) with MP4. Percent CO-Hb of the MP4 and blood samples before mixing (time = 0) and 30 min after mixing (time = 30 min) are displayed. CO, carbon monoxide.

compartments. In MP4→RBC, the [Hb] in the MP4 solution (~40 g L^{-1}) was one-fourth that of RBCs (~160 g L^{-1}), so that the final CO saturation of both Hb compartments reached approximately 25%. In the reverse reaction of RBC→MP4, CO-saturated RBCs were equilibrated with oxy-MP4, and the final saturation in both compartments was ~75%.

Rat model of myocardial infarct

Forty-eight animals completed the protocol and were analysed in the following groups: LR (13), oxy-MP4 (10), low-dose CO-MP4 (10), high-dose CO-MP4 (10) and PC (5). Five animals died between the time of treatment and 24-h recovery, which were not included in the analysis of data, distributed as follows: LR (2), oxy-MP4 (1), low-dose CO-MP4 (1) and high-dose CO-MP4 (1). Seventeen animals were excluded from analysis for technical reasons, including poor staining, surgical complications and instrumentation failure, as follows: LR (6), oxy-MP4 (5), low-dose CO-MP4 (2), high-dose CO-MP4 (4) and PC (2).

Table 2 shows pre-study and 24-h body weights, total Hb and percent CO-Hb at baseline, time of reperfusion and 24-h post-reperfusion. There were no statistically significant differences in body weight at baseline or 24-h post-reperfusion. Total Hb was similar in all groups of animals at baseline. There was a slight haemodilution over the 24 h of study as Hb fell in each of the groups. This haemodilution occurred more quickly (that is, at beginning of reperfusion) in CO-MP4 and oxy-MP4 treated groups, but Hb fell to similar levels in all groups at 24 h. The fraction of CO-Hb rose only in the CO-MP4 treated animals at the beginning of reperfusion (low dose, 5.2% and high dose, 7.6%) and was still slightly elevated from baseline 24 h later. Plasma Hb was undetectable at baseline and increased in oxy-MP4 (8 ± 0.1 g L^{-1}), low-dose CO-MP4 (8 ± 0.3 g L^{-1}) and high-dose CO-MP4 (12 ± 0.2 g L^{-1}) groups. Plasma Hb remained elevated at 24 h in oxy-MP4 (6 ± 0.1 g L^{-1}), low dose CO-MP4 (6 ± 0.1 g L^{-1}) and high-dose CO-MP4 (9 ± 0.2 g L^{-1}) groups.

Table 2 Body weights at baseline and 24 h of reperfusion, and total Hb and co-oximetry data at baseline, immediately at reperfusion, and 24 h of reperfusion

	LR	*Oxy-MP4 (30%)*	*CO-MP4 (30%)*	*CO-MP4 (50%)*	*PC*
Body weight (g)					
Baseline	285 ± 4	288 ± 5	285 ± 4	286 ± 4	300 ± 5
24 h	284 ± 3	287 ± 4	286 ± 5	286 ± 5	298 ± 6
Total Hb (g L^{-1})					
Baseline	169 ± 3	164 ± 2	164 ± 2	162 ± 1	161 ± 4
Reperfusion	153 ± 4[a]	139 ± 2[a,b]	139 ± 2[a,b]	122 ± 1[a,b]	156 ± 6
24 h	121 ± 3[a]	126 ± 3[a]	126 ± 3[a]	121 ± 3[a]	117 ± 4[a]
CO-Hb (%)					
Baseline	2.9 ± 0.2	2.5 ± 0.2	2.7 ± 0.1	2.5 ± 0.2	2.7 ± 0.3
Reperfusion	3.0 ± 0.2	2.5 ± 0.1	5.2 ± 0.2[a,b]	7.6 ± 0.2[a,b]	2.0 ± 0.7
24 h	3.2 ± 0.1	2.7 ± 0.5	3.6 ± 0.1[a]	3.6 ± 0.1[a]	3.0 ± 0.3

Abbreviations: CO, carbon monoxide; PC, preconditioning; LR, lactated Ringer's solution.
CO-MP4 30 and 50% designations refer to dosing volumes (see text for details).
[a]Denotes $P<0.05$ compared with baseline value.
[b]Denotes $P<0.0125$ compared with LR at the same time point.

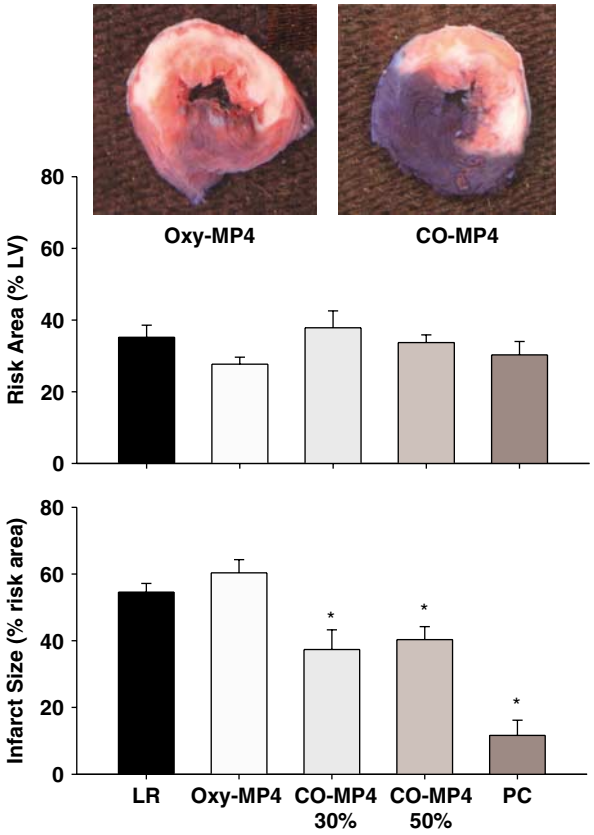

Figure 8 Top: representative digital photographs of heart slices from oxy-MP4 group (left) and CO-MP4 group (right) stained with Evans blue and TTC, followed by overnight immersion in formalin. Middle: myocardial area at risk (percent of total LV). Bottom: infarct size (percent of risk area). *denotes $P<0.0125$ versus LR group. CO, carbon monoxide; LR = lactated Ringer's solution only; LV, left ventricle; PC = preconditioning; TTC, triphenyl tetrazolium chloride.

Myocardial infarct size, arrhythmias and haemodynamics. Figure 8 shows the effect of treatment on area at risk and infarct size expressed as percent of area at risk. Area at risk was not different in any of the groups and averaged approximately 30% of the total left ventricle area. Analysis of covariance revealed that infarct size did not correlate with size of the area at risk, likely due to the uniformity in the size of risk area in all hearts. Infarct size in LR and oxy-MP4 treated rats was not different (P = NS versus LR), respectively. Infarct size was reduced equally ($P<0.0125$ versus LR) by treatment with low-dose CO-MP4 (37 ± 5.9%) and high-dose CO-MP4 (40 ± 4%). Thus, in the range of CO-Hb achieved in this study, the effects of CO on infarct size were not dose-dependent. PC reduced infarct size markedly to about 20% of that in the LR rats (12 ± 4.6%).

Arterial pH (7.39–7.46) and PCO_2 (35–45 mm Hg) remained within normal limits at all time points. There were no significant changes in mean arterial pressure, heart rate or core temperature at any time point in any of the groups (data not shown).

Discussion

This report is directed at the biochemical and pharmacological actions of CO-MP4 as a new CO delivery agent. Kinetic studies were carried out to evaluate MP4's ability to act as a CO as well as an O_2 carrier. Kinetic evaluation of O_2 binding to MP4 has been reported previously (Vandegriff *et al.*, 2004), but whereas O_2 combination is rate-limited by diffusion through protein cavities, CO combination is rate-limited by the reactivity of the haem iron, thus providing a more detailed picture of structure and energetics.

CO kinetic interpretation of MP4 structure and function
A previous study on O_2 binding kinetics led to the conclusion that MP4 is non-cooperative, with a molecular structure constrained in an intermediate conformation between T- and R-states (Vandegriff *et al.*, 2004). Overall, CO association time courses for MP4 are heterogeneous. By definition, the rate measured by the partial flash photolysis experiments reflects CO binding to 'R-state' Hb, resulting from the $Hb(CO)_3$ photolytic intermediate; the slower fitted rate observed with MP4 may be any of the following: (1) MP4

Table 3 Subunit assignments for the rate and equilibrium constants for the 'R state' and rate constants for 'T-state' of CO binding to MP4 and Hb

Hb	*Subunit*	k'_R ($\mu M^{-1}\,s^{-1}$)	k_R (s^{-1})	K_R (μM^{-1})	*Overall* K_R (μM^{-1})	k'_T ($\mu M^{-1}\,s^{-1}$)
Hb	α	2.9	0.019 ± 0.001	152	268	0.23 ± 0.01
	β	9.0		474		
MP4	α	4.1	0.022 ± 0.001	186	264	0.38 ± 0.04
	β	12.0	0.032 ± 0.003	375		4.44 ± 1.57

Subunit assignments were based on the fast and slow rates from Table 1, which were assigned to β and α subunits, respectively. 'R-state' dissociation rates are reported from the NO ligand displacement reactions in Table 1. The equilibrium constants for CO binding to the subunits with 'R-state' Hbs were calculated from the ratio of the rate constants, $K_R = k'_R\, k_R^{-1}$. Overall K_R was calculated as $K_R = (K_{R\alpha} \times K_{R\beta})^{1/2}$, according to Equation (4).

may provide a more highly photolyzed tetramer (for example, $Hb(CO)_2$); however, this interpretation is incompatible with stopped-flow experiments of CO binding to deoxy-MP4 in which a T→R transition was not observed. (2) The sample exhibits intermolecular heterogeneity, with a less reactive 'R-state' (perhaps molecules with variable numbers of PEG bound); or (3) the sample exhibits intramolecular heterogeneity, with a less reactive subunit within the same tetramer, such that the chemical modification increases the functional differences between α and β chains. As intermolecular heterogeneity will obscure any intramolecular effect, we cannot discriminate between cases 2 and 3, and both cases are compatible with the stopped-flow results for the 'T-state' association reactions. The observation of an 'R-state'-like rate for deoxy-MP4 suggests that the sample contains either a large fraction of dimers or 'R-state' tetramers, the latter being a fraction of molecules that are not in the 'T state' in the absence of ligands. Based on results for analysis of dimer formation at the MP4 concentration used in these kinetic experiments, it is unlikely that the 50:50 phase heterogeneity is due to enhanced dimerization.

As the CO reaction kinetics are heterogeneous, subunit cooperativity (in equilibrium experiments) and autocatalysis (in kinetic experiments) are hidden. Thus, a significant fraction of MP4 may be cooperative, but it becomes apparent only by comparison of stopped-flow and partial flash photolysis experiments, where it is slowly reacting in the former and quickly reacting in the latter. At the beginning of the combination of CO with 'T-state' MP4, autocatalysis is not observed because the reaction is masked by the reaction to the fraction of 'R-state' MP4.

As MP4 is a heterogeneous product, the rates do not refer to a well-defined molecular species but represent average quantities measured in a mixture of species, varying in number and sites of conjugated PEG chains. The solution kinetics may reflect either or both intra- and intermolecular heterogeneity. We have shown, however, in a small-angle X-ray scattering study that the MP4 structure remains intact upon PEGylation and has a core protein structure similar in size and shape to Hb, with PEG inside the internal Hb cavity and extending away from the surface, leading to an increase in particle size (Svergun *et al*., 2008). The absence of a CO geminate phase in MP4, as shown in Figure 1, may reflect the presence of PEG within the Hb molecule, such that steric hindrance inhibits CO rebinding in the haem pocket before it escapes to the solvent.

Support for intramolecular (that is, subunit) heterogeneity is shown by the kinetic phases tending toward equal amplitudes. Structural support for this interpretation comes from the fact that maleimidated β93Cys residues are immediately adjacent to β-subunit proximal histidines (β92His). Thus, it is likely that the reaction of βCys induces steric hindrance at β proximal His residues and haems. The assignment is further supported by a previous kinetic study of haem dissociation from met-MP4, showing higher rates of haem loss from β subunits compared to Hb, with unaltered α-chain kinetics (Vandegriff *et al*., 2006). This leads to an interpretation for the biphasic CO binding rates, with faster rates corresponding to reactions at β chains and slower rates to α chains. Based on these assignments, we predict that deoxygenated PEGylated β subunits are unable to convert from 'R state' to 'T state'; whereas, α chains may be less affected by PEGylation and are able to change tertiary conformation to a more deoxy T-like structure.

By making tentative assignments of kinetic rates to α and β subunits, rate and equilibrium constants for CO binding to individual subunits for Hb and MP4 are provided in Table 3. According to the kinetic constants for the individual subunits, the CO affinity assigned to 'R-state' β chains in either Hb or MP4 are two- to three-fold higher than those assigned to the α chains. The overall R-state CO equilibrium constants calculated by Equation 4 for Hb and MP4 are similar, 268 versus 264 μM^{-1}, respectively.

CO-MP4 is a storage-stable product

Currently, MP4 is prepared in an air-equilibrated environment and stored frozen, giving a product subject to oxidation and degradation *in vitro* (Figure 6) (Vandegriff *et al*., 2006). In contrast, CO-MP4 did not oxidize, and the percent met-Hb in the sample actually declined. The latter finding is consistent with earlier studies showing that CO reduces haem proteins, including met-Hb (Bickar *et al*., 1984).

CO-MP4 provides CO transport in vitro

The ability of MP4 to act as a CO carrier was shown *in vitro* by mixing CO-MP4 with blood. These data show that RBC-Hb and MP4 have similar partition constants for both O_2 and CO. The similar CO affinities shown in Table 3 are consistent with the equal distribution of CO-Hb concentrations between acellular Hb (MP4) and RBC-Hb compartments, thus showing that CO-MP4 is able to deliver CO to the circulation. The R-state affinities for O_2, as calculated from kinetic experiments of O_2 binding to MP4 or unmodified Hb,

are also similar (Vandegriff *et al*., 2004). The rate-limiting step for CO delivery is the 'R-state' off rate, giving an overall $t_{1/2}$ for the reaction of approximately 30–40 s. Thus, the 30-min equilibration study between CO-MP4 and RBCs was more than adequate to allow full CO re-distribution. In addition, the CO affinity of MP4 provides dissociation on a time scale that is much faster than the rate of MP4 clearance *in vivo*, that is, approximately 20 h in humans (Olofsson *et al*., 2006).

CO-MP4 is cardioprotective

We have demonstrated that intravenous administration of CO-MP4 limits infarct size in the rat in the absence of either hemodynamic actions or excessive elevation of circulating total CO-Hb. As oxy-MP4 did not provide cardioprotection, the effect is not due to increased oxygen delivery from the plasma Hb concentration achieved in this study.

There are now numerous studies documenting beneficial effects of CO in animal models of sickle cell disease (Belcher *et al*., 2006), heart (Akamatsu *et al*., 2004), kidney (Neto *et al*., 2004) and lung (Kohmoto *et al*., 2007) transplant, hemorrhage/resuscitation (Zuckerbraun *et al*., 2005), pulmonary injury (Ryter *et al*., 2007) and myocardial ischaemia (Fujimoto *et al*., 2004). Most of these studies utilized inhaled CO at levels between 250–1000 ppm for extended periods of time, and achieved CO-Hb saturation near 20% of total Hb. These levels of CO-Hb are generally considered toxic during chronic exposure (Mirza *et al*., 2005; Durante *et al*., 2006; Gautier *et al*., 2007) and, at the very least, will engage acute compensatory changes due to hypoxia when SaO_2 falls below 90% (Koehler *et al*., 1982). Although the dose-dependency of CO-mediated cytoprotection is not completely understood, evidence suggests inhaled CO is ineffective at concentrations that do not raise CO-Hb saturation. One study was unable to demonstrate a beneficial effect on survival of transplanted hearts after exposure to 20 ppm CO alone (Nakao *et al*., 2005), suggesting that inhaled CO resulting in CO-Hb saturation near 6% is ineffective. Lack of cardioprotection was also observed in rats with CO-Hb saturation below 25% (Fujimoto *et al*., 2004).

In contrast, our current results demonstrate that intravenous delivery of CO achieves beneficial effects without dramatic elevation of circulating CO-Hb concentration. In this regard, we calculate that the amount of CO gas administered by CO-MP4 in the current study ($\sim 13\,\mu mol\,kg^{-1}$) is similar to that delivered in the studies of Guo (Guo *et al*., 2004) and Stein (Stein *et al*., 2005), who demonstrated infarct reduction in mice using the prototype CO-releasing molecules ($\sim 11\,\mu mol\,kg^{-1}$). To our knowledge, there are no studies that describe the relationship between circulating CO-Hb concentration, tissue CO concentration and the cytoprotective effects of CO. Together with the actions of CO-releasing molecules (Guo *et al*., 2004; Stein *et al*., 2005), our results suggest that CO administered intravenously by carrier molecules might be more targeted to tissue by avoiding the systemic exposure inherent in inhaled delivery.

The role of CO in the cardioprotection with CO-MP4 is indicated by the observation that infarct size was not reduced by an equivalent administration of oxy-MP4. Moreover, the *in vitro* partitioning studies demonstrate rapid equilibration of CO with red blood cell Hb and suggest that some portion of the CO released from MP4 is also available to bind to tissues. The observation by Guo (Guo *et al*., 2004) and Stein (Stein *et al*., 2005) that CO-releasing molecules impart cardioprotection without a measurable increment of CO-Hb in the blood implies that the mechanism responsible is very sensitive and can be activated by low circulating levels of CO. This concept is supported by the current observation that the cardioprotection was not improved by doubling the infused dose of CO-MP4 over the 24-h period (Figure 8). However, despite extensive recent progress (Bilban *et al*., 2008), the mechanisms of cytoprotection by CO remain undetermined. The vasoactive actions of CO have been recognized for some time (Sammut *et al*., 1998; Motterlini *et al*., 2002) and could contribute to improved perfusion. In addition, the creation of a 'preconditioned' phenotype in myocardium by CO (Stein *et al*., 2005) evokes a number of potential cardioprotective actions, including generation of reactive oxygen species (Yellon and Downey, 2003; Cohen *et al*., 2006; Bilban *et al*., 2008) and activation of effector mechanisms such as K^+ channel opening (Clark *et al*., 2003; Dong *et al*., 2007), stabilization of HIF-1α (Ockaili *et al*., 2005; Natarajan *et al*., 2006; Chin *et al*., 2007) and induction of cardioprotective proteins (Yellon and Downey, 2003; Dawn and Bolli, 2005; Bilban *et al*., 2008). The effects of MP4, with regard to these potential mechanisms, are only speculative at this point. Future studies will determine the tissue distribution of CO delivered by CO-MP4 and further explore the dose-response relationship and cell signalling pathways responsible for its actions.

Acknowledgements

This work was supported by the National Institutes of Health Bioengineering Partnership Grant R24 64395, NHLBI Grant R01 076163 and by Grant CE LSHB-CT-2004-505023 'Euro-BloodSubstitutes'. We thank Professor Maurizio Brunori, Department of Biochemical Sciences, University of Rome ''La Sapienza, for his helpful comments on this manuscript.

Conflict of interest

KD Vandegriff, A Malavalli, MA Young, J Lohman and RM Winslow, are employees of Sangart, Inc. and hold stock options in the company. Dr Winslow is President, CEO and Chairman of the Board of Sangart, Inc.

References

Acharya AS, Manjula BN, Smith P (1996). Hemoglobin crosslinkers. US Patent number 5, 585, 484.

Akamatsu Y, Haga M, Tyagi S, Yamashita K, Graca-Souza AV, Ollinger R *et al.* (2004). Heme oxygenase-1-derived carbon monoxide protects hearts from transplant associated ischemia reperfusion injury. *FASEB J* **18**: 771–772.

Belcher JD, Mahaseth H, Welch TE, Otterbein LE, Hebbel RP, Vercellotti GM (2006). Heme oxygenase-1 is a modulator of inflammation and vaso-occlusion in transgenic sickle mice. *J Clin Invest* **116**: 808–816.

Bickar D, Bonaventura C, Bonaventura J (1984). Carbon monoxide-driven reduction of ferric heme and heme proteins. *J Biol Chem* **259**: 10777–10783.

Bilban M, Haschemi A, Wegiel B, Chin BY, Wagner O, Otterbein LE (2008). Heme oxygenase and carbon monoxide initiate homeostatic signaling. *J Mol Med* **86**: 267–279.

Björkholm M, Fagrell B, Przybelski R, Winslow N, Young M, Winslow RM (2005). A phase I single blind clinical trial of a new oxygen transport agent (MP4), human hemoglobin modified with maleimide-activated polyethylene glycol. *Haematologica* **90**: 505–515.

Chin BY, Jiang G, Wegiel B, Wang HJ, Macdonald T, Zhang XC *et al*. (2007). Hypoxia-inducible factor 1 alpha stabilization by carbon monoxide results in cytoprotective preconditioning. *Proc Natl Acad Sci USA* **104**: 5109–5114.

Clark JE, Naughton P, Shurey S, Green CJ, Johnson TR, Mann BE *et al*. (2003). Cardioprotective actions by a water-soluble carbon monoxide-releasing molecule. *Circ Res* **93**: e2–e8.

Cohen MV, Yang XM, Downey JM (2006). Nitric oxide is a preconditioning mimetic and cardioprotectant and is the basis of many available infarct-sparing strategies. *Cardiovasc Res* **70**: 231–239.

Dawn B, Bolli R (2005). HO-1 induction by HIF-1: a new mechanism for delayed cardioprotection? *Am J Physiol Heart Circ Physiol* **289**: H522–H524.

Dong DL, Zhang Y, Lin DH, Chen J, Patschan S, Goligorsky MS *et al*. (2007). Carbon monoxide stimulates the $Ca^{2(+)}$-activated big conductance k channels in cultured human endothelial cells. *Hypertension* **50**: 643–651.

Durante W, Johnson FK, Johnson RA (2006). Role of carbon monoxide in cardiovascular function. *J Cell Mol Med* **10**: 672–686.

Foresti R, Hammad J, Clark JE, Johnson TR, Mann BE, Friebe A *et al*. (2004). Vasoactive properties of CORM-3, a novel water-soluble carbon monoxide-releasing molecule. *Br J Pharmacol* **142**: 453–460.

Fujimoto H, Ohno M, Ayabe S, Kobayashi H, Ishizaka N, Kimura H *et al*. (2004). Carbon monoxide protects against cardiac ischemia—reperfusion injury *in vivo* via MAPK and Akt—eNOS pathways. *Arterioscler Thromb Vasc Biol* **24**: 1848–1853.

Gautier M, Antier D, Bonnet P, Le Net JL, Hanton G, Eder V (2007). Continuous inhalation of carbon monoxide induces right ventricle ischemia and dysfunction in rats with hypoxic pulmonary hypertension. *Am J Physiol Heart Circ Physiol* **293**: H1046–H1052.

Guo Y, Stein AB, Wu WJ, Tan W, Zhu X, Li QH *et al*. (2004). Administration of a CO-releasing molecule at the time of reperfusion reduces infarct size *in vivo*. *Am J Physiol Heart Circ Physiol* **286**: H1649–H1653.

Khan I, Dantsker D, Samuni U, Friedman AJ, Bonaventura C, Manjula B *et al*. (2001). β93 Modifiied hemoglobin: kinetic and conformational consequences. *Biochemistry* **40**: 7581–7592.

Koehler RC, Jones Jr MD, Traystman RJ (1982). Cerebral circulatory response to carbon monoxide and hypoxic hypoxia in the lamb. *Am J Physiol* **243**: H27–H32.

Kohmoto J, Nakao A, Stolz DB, Kaizu T, Tsung A, Ikeda A *et al*. (2007). Carbon monoxide protects rat lung transplants from ischemia-reperfusion injury via a mechanism involving p38 MAPK pathway. *Am J Transplant* **7**: 2279–2290.

Kubulus D, Rensing H, Paxian M, Thierbach JT, Meisel T, Redl H *et al*. (2005). Influence of heme-based solutions on stress protein expression and organ failure after hemorrhagic shock. *Crit Care Med* **33**: 629–637.

Kusuoka H, Hoffman JIE (2002). Advice on statistical analysis for circulation research. *Circ Res* **91**: 662–671.

Mathews AJ, Olson JS (1994). Assignment of rate constants for O_2 and CO binding to α and β subunits within R- and T-state human hemoglobin. *Meth Enzymol* **232**: 363–386.

Mathews AJ, Olson JS, Renaud JP, Tame J, Nagai K (1991). The assignment of carbon monoxide association rate constants to the alpha and beta subunits in native and mutant human deoxyhemoglobin tetramers. *J Biol Chem* **266**: 21631–21639.

Mathews AJ, Rohlfs RJ, Olson JS, Tame J, Renaud JP, Nagai K (1989). The effects of E7 and E11 mutations on the kinetics of ligand binding to R-state human hemoglobin. *J Biol Chem* **264**: 16573–16583.

Mirza A, Eder V, Rochefort GY, Hyvelin JM, Machet MC, Fauchier L *et al*. (2005). CO inhalation at dose corresponding to tobacco smoke worsens cardiac remodeling after experimental myocardial infarction in rats. *Toxicol Sci* **85**: 976–982.

Motterlini R, Clark JE, Foresti R, Sarathchandra P, Mann BE, Green CJ (2002). Carbon monoxide-releasing molecules: characterization of biochemical and vascular activities. *Circ Res* **90**: E17–E24.

Nakao A, Kimizuka K, Stolz DB, Neto JS, Kaizu T, Choi AM *et al*. (2003). Carbon monoxide inhalation protects rat intestinal grafts from ischemia/reperfusion injury. *Am J Pathol* **163**: 1587–1598.

Nakao A, Neto JS, Kanno S, Stolz DB, Kimizuka K, Liu F *et al*. (2005). Protection against ischemia/reperfusion injury in cardiac and renal transplantation with carbon monoxide, biliverdin and both. *Am J Transplant* **5**: 282–291.

Natarajan R, Salloum FN, Fisher BJ, Kukreja RC, Fowler III AA (2006). Hypoxia inducible factor-1 activation by prolyl 4-hydroxylase-2 gene silencing attenuates myocardial ischemia reperfusion injury. *Circ Res* **98**: 133–140.

Neto JS, Nakao A, Kimizuka K, Romanosky AJ, Stolz DB, Uchiyama T *et al*. (2004). Protection of transplant-induced renal ischemia-reperfusion injury with carbon monoxide. *Am J Physiol Renal Physiol* **287**: F979–F989.

Ockaili R, Natarajan R, Salloum F, Fisher BJ, Jones D, Fowler III AA *et al*. (2005). HIF-1 activation attenuates postischemic myocardial injury: role for heme oxygenase-1 in modulating microvascular chemokine generation. *Am J Physiol Heart Circ Physiol* **289**: H542–H548.

Olofsson C, Ahl T, Johansson T, Larsson S, Nellgård P, Ponzer S *et al*. (2006). A multi-center clinical study of the safety and activity of maleimide-polyethylene glycol hemoglobin (Hemospan®) in patients undergoing major orthopedic surgery. *Anesthesiology* **105**: 1153–1163.

Olofsson C, Nygårds EB, Ponzer S, Fagrell B, Przybelski R, Keipert PE *et al*. (2008). A randomized, single blind, increasing dose safety trial of an oxygen-carrying plasma expander (Hemospan®) administered to orthopedic surgery patients with spinal anesthesia. *Transfusion Med* **18**: 28–39.

Otterbein LE (2002). Carbon monoxide: innovative anti-inflammatory properties of an age-old gas molecule. *Antioxid Redox Signal* **4**: 309–319.

Ryter SW, Kim HP, Nakahira K, Zuckerbraun BS, Morse D, Choi AM (2007). Protective functions of heme oxygenase-1 and carbon monoxide in the respiratory system. *Antioxid Redox Signal* **9**: 2157–2173.

Samaja M, Rovida E, Niggeler M, Perrella M, Rossi-Bernardi L (1987). The dissociation of carbon monoxide from hemoglobin intermediates. *J Biol Chem* **262**: 4528–4533.

Sammut IA, Foresti R, Clark JE, Exon DJ, Vesely MJ, Sarathchandra P *et al*. (1998). Carbon monoxide is a major contributor to the regulation of vascular tone in aortas expressing high levels of haeme oxygenase-1. *Br J Pharmacol* **125**: 1437–1444.

Sawle P, Foresti R, Mann BE, Johnson TR, Green CJ, Motterlini R (2005). Carbon monoxide-releasing molecules (CO-RMs) attenuate the inflammatory response elicited by lipopolysaccharide in RAW264.7 murine macrophages. *Br J Pharmacol* **145**: 800–810.

Sharma VS, Ranney HM (1982). Studies on hemoglobin intermediates. A new method for studying the reaction Hb4(CO)3 with CO in human, carp, rabbit and opossum hemoglobin. *J Mol Biol* **158**: 551–558.

Snell SM, Marini MA (1988). A convenient spectroscopic method for the estimation of hemoglobin concentrations in cell-free solutions. *J Biochem Biophys Meth* **17**: 25–33.

Stein AB, Guo Y, Tan W, Wu WJ, Zhu X, Li Q *et al*. (2005). Administration of a CO-releasing molecule induces late preconditioning against myocardial infarction. *J Mol Cell Cardiol* **38**: 127–134.

Svergun DI, Ekström F, Vandegriff KD, Malavalli A, Baker DA, Nilsson C *et al*. (2008). Molecular structure and interaction of poly(ethylene) glycol-conjugated hemoglobin from solution X-ray

scattering: implications for a new oxygen therapeutic. *Biophys J* **94**: 173–181.

Unzai S, Eich R, Shibayama N, Olson JS, Morimoto H (1998). Rate constants for O_2 and CO binding to the α and β subunits within the R and T states of human hemoglobin. *J Biol Chem* **273**: 23150–23159.

Vandegriff KD, Bellelli A, Samaja M, Malavalli A, Brunori M, Winslow RM (2004). Kinetics of NO and O_2 binding to a maleimide poly(ethylene glycol)-conjugated human haemoglobin. *Biochem J* **382**: 183–189.

Vandegriff KD, Malavalli A, Mann C, Jiang E, Lohman J, Young MA *et al.* (2006). Oxidation and haeme loss kinetics of poly(ethylene glycol)-conjugated hemoglobin (MP4): dissociation between *in vitro* and *in vivo* oxidation rates. *Biochem J* **399**: 463–471.

Vandegriff KD, Malavalli A, Wooldridge J, Lohman J, Winslow RM (2003). MP4, a new nonvasoactive PEG-Hb conjugate. *Transfusion* **43**: 509–516.

Yellon DM, Downey JM (2003). Preconditioning the myocardium: from cellular physiology to clinical cardiology. *Physiol Rev* **83**: 1113–1151.

Zuckerbraun BS, McCloskey CA, Gallo D, Liu F, Ifedigbo E, Otterbein LE *et al.* (2005). Carbon monoxide prevents multiple organ injury in a model of hemorrhagic shock and resuscitation. *Shock* **23**: 527–532.